Chalcogenol Ligand Toolbox for CdSe Nanocrystals and Their Influence on Exciton Relaxation Pathways

Jannise J. Buckley,[†,§] Elsa Couderc,[†,§] Matthew J. Greaney,[†] James Munteanu,[†] Carson T. Riche,[‡] Stephen E. Bradforth,[†,*] and Richard L. Brutchey[†,*]

[†]Department of Chemistry and the Center for Energy Nanoscience, University of Southern California, Los Angeles, California 90089, United States, and [‡]Mork Family Department of Chemical Engineering and Materials Science, University of Southern California, Los Angeles, California 90089, United States. [§]These authors contributed equally to this work.

ABSTRACT We have employed a simple modular approach to install small chalcogenol ligands on the surface of CdSe nanocrystals. This versatile modification strategy provides access to thiol, selenol, and tellurol ligand sets *via* the *in situ* reduction of R_2E_2 (R = ^{t}Bu, Bn, Ph; E = S, Se, Te) by diphenylphosphine (Ph_2PH). The ligand exchange chemistry was analyzed by solution NMR spectroscopy, which reveals that reduction of the R_2E_2 precursors by Ph_2PH directly yields active chalcogenol ligands that subsequently bind to the surface of the CdSe nanocrystals. Thermogravimetric analysis, FT-IR spectroscopy, and energy dispersive X-ray spectroscopy provide further evidence for chalcogenol addition to the CdSe surface with a concomitant reduction in overall organic content from the displacement of native ligands. Time-resolved and low temperature photoluminescence measurements showed that all of the phenylchalcogenol ligands rapidly quench the photoluminescence by hole localization onto the ligand. Selenol and tellurol ligands exhibit a larger driving force for hole transfer than thiol ligands and therefore quench the photoluminescence more efficiently. The hole transfer process could lead to engineering long-lived, partially separated excited states.

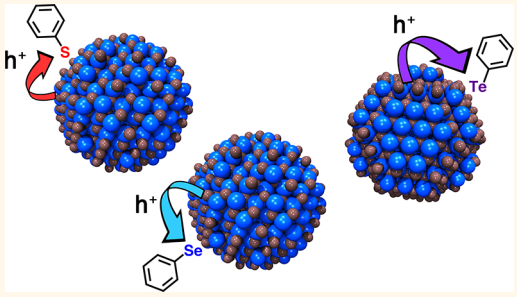

KEYWORDS: CdSe · quantum dot · ligand exchange · nanocrystals · photoluminescence

The optoelectronic properties of colloidal semiconductor nanocrystals are largely dependent on their surface chemistry as a result of their large surface-to-volume ratios.[1−4] While the native ligands that are installed during nanocrystal synthesis impart solution dispersibility and may passivate surface trap states, these ligands are typically long-chain aliphatic compounds that are also electrically insulating (*e.g.*, C18 fatty acids like stearic acid), and they therefore have an extremely detrimental effect on conductivity and charge mobility in nanocrystal-based thin film devices.[5,6] As a result, there is currently a tremendous amount of interest in controlling the surface chemistry of colloidal semiconductor nanocrystals *via* ligand exchange approaches.[5,7,8] In such an approach, the native ligands are exchanged with less sterically demanding ligands that ideally still impart solution dispersibility and effectively passivate the nanocrystal surface, but which also allow for more efficient interparticle charge transfer in nanocrystal thin film devices.

The CdSe nanocrystal surface is generally cadmium-rich,[9,10] which necessitates charge balance with an anionic X-type ligand.[11,12] Much success has been had with ligand exchanges that employ both strong and weakly coordinating inorganic X-type anions, such as chloride,[13] thiocyanate,[14] sulfide,[15−17] chalcogenometallates,[18] and tetrafluoroborate;[19,20] however, less success has been achieved with small organic ligands. Traditionally, organic ligand exchanges have been done with pyridine and small primary amines,[21−24] but such neutral L-type ligands cannot exchange the strongly bound X-type ligands on nonstoichiometric nanocrystal surfaces unless there is some degree of surface reconstruction (*e.g.*, through loss of CdX_2).[11] We previously reported that *tert*-butylthiol could be employed as a small organic ligand to quantitatively displace native long-chain carboxylate and phosphonate ligands on CdSe nanocrystals and

* Address correspondence to brutchey@usc.edu, bradfort@usc.edu.

Received for review November 26, 2013 and accepted February 5, 2014.

Published online February 05, 2014
10.1021/nn406109v

yield colloidally stable dispersions.[25] After ligand exchange with *tert*-butylthiol, a significant decrease in organic content was observed by thermogravimetric analysis (TGA) and FT-IR spectroscopy. Importantly, ligand exchange with *tert*-butylthiol leads to significantly improved photocurrent, charge mobility, and power conversion efficiencies in nanocrystal-based devices relative to those using nonligand-exchanged or pyridine-exchanged CdSe nanocrystals.[25−27] In addition to affecting quantitative ligand exchange of both X-type and L-type ligands, it is known that soft thiol ligands bind very strongly to the soft cadmium atoms on the surface of CdSe.[28,29] From this, it follows that the analogous selenols and tellurols would also be expected to have a strong binding affinity for CdSe nanocrystal surfaces as a result of their chemically soft nature. To the best of our knowledge, however, there have been no studies on the binding of organotellurol ligands to CdSe nanocrystals, and only one descriptive example of phenylselenolate binding to CdSe clusters using $PhSeSiMe_3$ in 1988.[30] Thus, there is interest in developing simple, modular approaches for the installation of selenol and tellurol ligands onto CdSe nanocrystals such that the fundamental ligand exchange chemistry and photophysics may be studied on these systems and compared to that of traditional thiol ligands.

The photophysical study of nanocrystals offers an experimental window into their electronic structure and into the fate of photogenerated charge carriers. Energetic positions of the conduction and valence band edges are determined by the material and size of the nanocrystal, due to quantum confinement effects, resulting in tunable absorption and emission properties. The positions of the band edge levels relative to that of the surrounding molecules or lack thereof (*e.g.*, surface states created by dangling Cd or Se bonds) also affect the oxidative and reductive abilities of the nanocrystals. Positively or negatively doping nanocrystals *via* charge transfer to the ligands modifies the emission characteristics of the nanocrystals by competing with other radiative and nonradiative pathways, and conversely, the nanocrystal emission offers an opportunity to study charge transfer processes and dynamics. The influence of thiol ligands on the photophysical properties of CdSe nanocrystals has been extensively studied; transient absorption and photoluminescence (PL) studies have shown that thiol and thiolate ligands act as photogenerated hole traps and passivate electron traps.[31,32] On the other hand, the influence of selenol and tellurol ligands is much less explored to date. Recently, PbSe nanocrystals with a native oleate ligand shell were subjected to a ligand exchange with long-chain octyldecylselenol, which was shown to bind to the nanocrystal surface as selenolate through a proton transfer mechanism with release of free oleic acid.[33] Investigation into the photophysical properties resulting from octyldecylselenol treatment on PbSe revealed the introduction of a new nonradiative decay pathway, identified as a hole-trap; similar effects have been observed after selenide (Se^{2-}) treatment of CdSe.[3]

Herein, we report a simple and modular ligand exchange procedure to replace native stearate ligands on CdSe nanocrystals using a full series of seven small, air-stable R_2E_2 dichalcogenide precursors (R = ^{t}Bu, E = Se or Te; R = Bn, E = S or Se; R = Ph, E = S, Se, or Te). This ligand exchange is accomplished by the reduction of the R_2E_2 dichalcogenide with diphenylphosphine (Ph_2PH) to generate the small chalcogenol ligand *in situ* in a CdSe nanocrystal suspension. Upon workup, this approach yields colloidally stable, thiol-, selenol-, or tellurol-exchanged nanocrystals whose low temperature and time-resolved photophysics were studied and compared. We show that four processes compete for the relaxation of photoexcitations: (i) band-edge emission, (ii) phonon-assisted nonradiative relaxation processes, (iii) surface state trapping, and finally, (iv) hole trapping by phenylchalcogenol ligands. While the importance of these processes depends on the temperature and ligand type, our findings show hole trapping to be more efficient for the phenylselenol and phenyltellurol ligands than for phenylthiol. For these ligands, the hole trapping mechanism could outcompete relaxation to the ground state *via* surface state trapping. This finding could help in the engineering of long-lived, partially separated excited states.

RESULTS AND DISCUSSION

Colloidal Ligand Exchange. The CdSe nanocrystals were synthesized *via* the hot injection of tri-*n*-octylphosphine selenide (TOPSe) into a solution of $Cd(stearate)_2$ in tri-*n*-octylphosphine oxide (TOPO, 98%) and technical grade stearic acid.[34] The resulting nanocrystals were purified three times using toluene as a dispersant and ethanol as a flocculant, with the final product being dispersed in toluene. The UV−vis spectrum of the resulting nanocrystals dispersed in toluene displayed a clear first exciton peak at 586 nm (2.12 eV), which is indicative of a CdSe nanocrystal diameter of 4.0 nm.[35] Transmission electron microscopy (TEM) revealed the CdSe nanocrystals to possess a spherical nanoparticle morphology with diameters of 3.9 ± 0.5 nm, which is in close agreement with empirical sizing by UV−vis spectroscopy.

The nanocrystals with the native ligand shell, CdSe(NL), can be ligand exchanged with seven R_2E_2 dichalcogenide precursors (R = ^{t}Bu, E = Se or Te; R = Bn, E = S or Se; R = Ph, E = S, Se, or Te) using a facile, one-step, room temperature reduction with Ph_2PH to generate the corresponding chalcogenol. Addition of R_2E_2 (0.30 mmol) and Ph_2PH (0.92 mmol) to a stirred suspension of CdSe(NL) nanocrystals in toluene (1.0 mL at a gravimetrically determined concentration of 17 mg mL^{-1} corrected to pure CdSe content based on the 500 °C

TGA mass) resulted in ligand exchange, as indicated by nanocrystal precipitation from the nonpolar solvent system. Ligand exchange reactions were performed under nitrogen using standard Schlenk techniques; however, the nanocrystals were handled in air post ligand exchange. Large differences in the reaction rates were observed for the ditellurides, diselenides, and disulfides. Addition of the ditellurides (*i.e.*, $^{t}Bu_2Te_2$ and Ph_2Te_2) in the presence of Ph_2PH to a CdSe(NL) suspension resulted in immediate nanocrystal precipitation, the diselenides (*i.e.*, $^{t}Bu_2Se_2$, Bn_2Se_2, and Ph_2Se_2) required a several hours (*ca.* 4 h) before nanocrystal precipitation, and the disulfides (*i.e.*, Bn_2S_2 and Ph_2S_2) gradually precipitated the nanocrystals over a 24 h period. Removal of excess precursors, reaction byproducts, and displaced native ligands required a total of four washes using tetramethylurea (TMU) as the dispersant and pentane as a flocculant.

The dispersibility of the CdSe nanocrystals was found to drastically change after ligand exchange. The CdSe(NL) nanocrystals are soluble in low polarity solvents, such as toluene and hexanes, as a result of the long-chain aliphatic native ligands. Replacement of the native ligands for smaller *tert*-butyl-, benzyl-, or phenylchalcogenols causes the nanocrystals to lose colloidal stability in nonpolar solvents; however, after ligand exchange the CdSe nanocrystals are readily dispersible in moderately polar solvents, such as TMU. Nanocrystal suspensions in TMU maintained high colloidal stability (>3 months), were optically transparent and were easily passed through a 100 nm filter. Additionally, it should be noted for optical studies that the line width of the first exciton peak remains unchanged after ligand exchange and washing indicating that the nanocrystal size population is similarly unchanged. While TMU proved to be the best solvent for these systems, they were also readily dispersible in other donor solvents, such as dimethyl sulfoxide (DMSO), *N*,*N*-dimethylacetamide (DMAc), and pyridine. The ligand exchanged CdSe nanocrystals were also dispersible in less polar solvents, such as 1,2-dichlorobenzene.

NMR Characterization. Multinuclear ^{1}H, ^{31}P, and ^{77}Se NMR spectroscopy was used to gain insight into the nature of the native ligands and their ligand exchange with the chalcogenols generated by *in situ* reduction. The conditions used to synthesize the CdSe nanocrystals in this study are known to produce native ligand shells primarily comprising stearate.[25] To verify this, NMR spectra were recorded for both the surface-bound native ligands and free native ligands from acid digested nanocrystals. The ^{1}H NMR spectrum of the purified CdSe(NL) nanocrystals in a $CDCl_3$ suspension displayed only the characteristic resonances of bound stearate ligands at 0.94, 1.28, and 1.60 ppm (see the Supporting Information, Figure S1). These NMR resonances display the typical broadening and downfield chemical shifts of surface bound species, with the α-methylene protons of the carbonyl group being essentially unobservable as a result of their proximity to the binding headgroup.[36−38] The native ligands were further analyzed after a typical digestion and extraction procedure using aqua regia.[18] The ^{1}H and ^{31}P NMR spectra in benzene-d_6 of the liberated ligands suggest that the CdSe(NL) surface is free of any detectable alkylphosphonic acid species and is ligated solely by stearic acid (δ = 0.92, 1.35, 1.47, 2.04 ppm) (see the Supporting Information, Figure S2).

The ligand exchange chemistry was monitored using multinuclear NMR spectroscopy; the stepwise addition of the reagents to benzene-d_6 elucidated the reduction and ligand exchange with Ph_2Se_2 as a model system (Figure 1). The reaction between Ph_2Se_2 and Ph_2PH (25 °C, 24 h) produced two products shown in Figure 1a,b, unambiguously identified as Ph_2PSePh (^{77}Se δ = 308.8 ppm; ^{31}P δ = 29.9 ppm (d, $^{1}J_{P-Se}$ = 229 Hz); m/z = 341.99) and PhSeH (^{77}Se δ = 145.5 ppm; ^{1}H δ = 1.26 (s), 7.16 (m) ppm; m/z = 157.99) by NMR spectroscopy and mass spectrometry.[39] Subsequent addition of CdSe(NL) nanocrystals to the same reaction of Ph_2Se_2 and Ph_2PH in benzene-d_6 (25 °C, 24 h) resulted in binding of the *in situ* generated PhSeH, as evidenced by the near complete disappearance of the sharp selenol resonances (^{77}Se δ = 145.5 ppm; ^{1}H δ = 1.26 ppm) and the broadening of the associated aromatic ^{1}H NMR signal at δ = 7.17 (Figure 1a,b; see the Supporting Information, Figures S3−S5). The appearance of a broad resonance (*i.e.*, ^{1}H δ = 2.7−3.0 ppm) that is present upfield from the unbound selenol Se−H resonance also suggests binding of the selenol ligand (Figure 1a; see the Supporting Information, Figure S6). Analogous NMR studies involving the addition of free thiols to CdSe nanocrystals have reported similar resonances for the sulfhydryl proton that appear broadened and shifted upfield from the free ligands; these signature resonances are attributed to bound thiols.[11] In addition, the release of a small amount of free stearic acid was observed by ^{1}H NMR spectroscopy (see the Supporting Information, Figure S6), presumably resulting from a proton transfer exchange mechanism occurring between the selenol and stearate on the CdSe nanocrystal surface.[33] Given the stronger acidic character of phenylselenol compared to stearic acid (pK_a = 10.15 for stearic acid in H_2O; pK_a = 5.9 for phenylselenol in H_2O), the equilibrium is expected to shift toward the formation of the selenolate.[40,41] Therefore, the NMR evidence suggests that the ligand may be binding as mixture of neutral L-type selenol and anionic X-type selenolate to the CdSe nanocrystal surface, as was previously proposed for the *tert*-butylthiol ligand.[25]

Efficacy of Ligand Exchange. Thermogravimetric analysis was used as one means of determining the degree of ligand exchange on the CdSe nanocrystal surface. The TGA traces (ambient to 500 °C, 10 °C min^{-1}, under flowing nitrogen) of the ligand exchanged nanocrystals

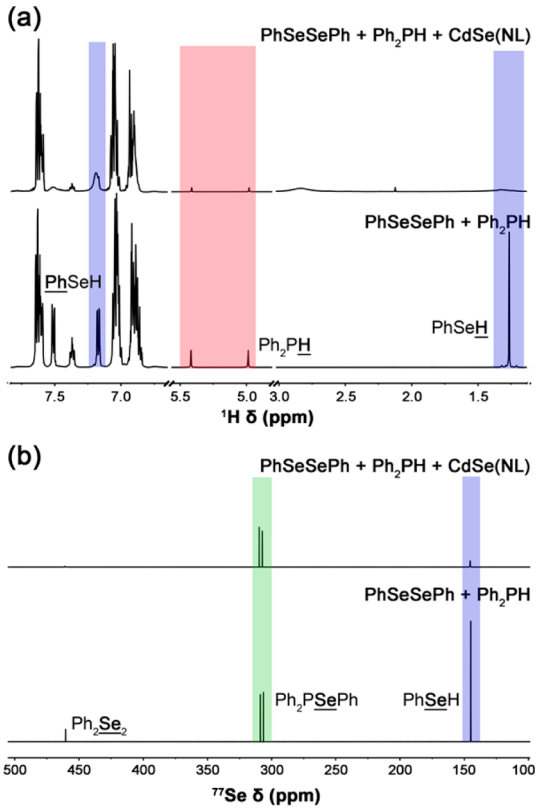

Figure 1. (a) ^{1}H and (b) ^{77}Se NMR spectra of the reaction between Ph_2Se_2 and Ph_2PH before and after the addition of CdSe(NL) nanocrystals. Full ^{1}H NMR spectra from 0 to 8 ppm are provided in the Supporting Information (Figure S3).

previously dried at 100 °C show a clear reduction in the total organic mass content when compared to the CdSe(NL) nanocrystals (Figure 2a; see the Supporting Information, Figure S7). By approximating the mass at 500 °C to be pure CdSe, it was found that dried CdSe(NL) nanocrystals contained 28% organic content after three toluene/ethanol washes. Ligand exchange reduces the total organic content by half (on average) and produces a new lower temperature (<300 °C) mass loss event, which likely corresponds to loss of the new chalcogenol ligands.[25]

To quantify the extent of ligand exchange by TGA, it was assumed that mass loss events >300 °C correspond to the tightly bound native stearate ligands (based on the TGA trace for the CdSe(NL) nanocrystal sample and previous work), while all new mass loss occurring <300 °C was attributed to the new chalcogenol ligands.[25] It should be noted that the chalcogenol ligands may also contribute to mass loss >300 °C; however, the majority of chalcogenol decomposition was assumed to be <300 °C for this analysis. Corroborating analyses show this to be a reasonable approximation (*vide infra*). For the CdSe(NL) nanocrystals, there is 0.39 g organics/g CdSe. The organic component is comprised of stearate, as discussed previously, with a mass loss event between 300−500 °C. For PhSH-exchanged CdSe nanocrystals, the 300−500 °C mass loss represents 0.08 g per gram of CdSe, corresponding to an 80% reduction in the stearate mass content. In the case of the PhSeH- and PhTeH-exchanged CdSe nanocrystals, the native ligand content is reduced by 70 and 79%, respectively. The mass loss below 300 °C is attributed to the new phenylchalcogenol ligands and represents 0.06 g per gram of CdSe for PhSH, 0.07 g per gram of CdSe for PhSeH, and 0.08 g per gram of CdSe for PhTeH ligands. The relative mass contributions of native stearate and of new ligands after ligand exchange with the entire series of dichalcogenide precursors studied are given in Table S1.

FT-IR spectroscopic analysis of the CdSe nanocrystals before and after ligand exchange with the phenylchalcogenols further validates the TGA data by showing large reductions in the native ligand content and the appearance of new bands corresponding to aromatic ν(C−H) stretches, as shown in Figure 2b. Quantitative comparisons were made possible through the use of an internal standard. All nanocrystal samples were dried at 100 °C before analysis, and all spectra were normalized in intensity to the 2089 cm^{-1} ν(C≡N) stretching peak of a $Fe_4[Fe(CN)_6]_3$ internal standard (see Experimental Methods). The normalized integrated areas under the aliphatic ν(C−H) stretching region were used to quantify removal of native ligands after ligand exchange since the aromatic stretching bands associated with the phenylchalcogenol ligands at ∼3050 cm^{-1} are well resolved from the ν(C−H) stretches associated with the native ligands in the range of 2800−3000 cm^{-1}. Ligand exchange using the Ph_2S_2, Ph_2Se_2, and Ph_2Te_2 dichalcogenide precursors resulted in a 79%, 73%, and 84% reduction in native ligand content, respectively; these data are in good agreement with TGA results. Reductions in the native ligand ν(C−H) stretching intensity were also observed after ligand exchange with the Bn_2E_2 and $^{t}Bu_2E_2$ dichalcogenide precursors, but quantification was not performed because the *tert*-butyl and benzyl groups of the entering ligands possess aliphatic C−H bonds. In general, however, it was qualitatively observed by FT-IR spectroscopy that these *tert*-butyl and benzylchalcogenol ligands also successfully displaced a large percentage of the native ligands, which is consistent with TGA results. Energy dispersive X-ray spectroscopy (EDX) further corroborated the presence of sulfur and tellurium after exchange with the PhSH and PhTeH ligands, respectively (Figure 2c). In contrast, the CdSe(NL) nanocrystals do not possess any sulfur or tellurium by EDX.

TEM analysis also provides evidence for ligand exchange when utilizing the heavier, and therefore more "visible" or electron-dense, tellurol ligands (see the Supporting Information, Figure S8). As previously stated, the average diameter of the CdSe(NL) nanocrystals measured in ImageJ from representative TEM micrographs was 3.9 ± 0.5 nm. After ligand exchange with the PhTeH or ^{t}BuTeH ligands, it was evident that the mean CdSe nanocrystal diameter had increased.

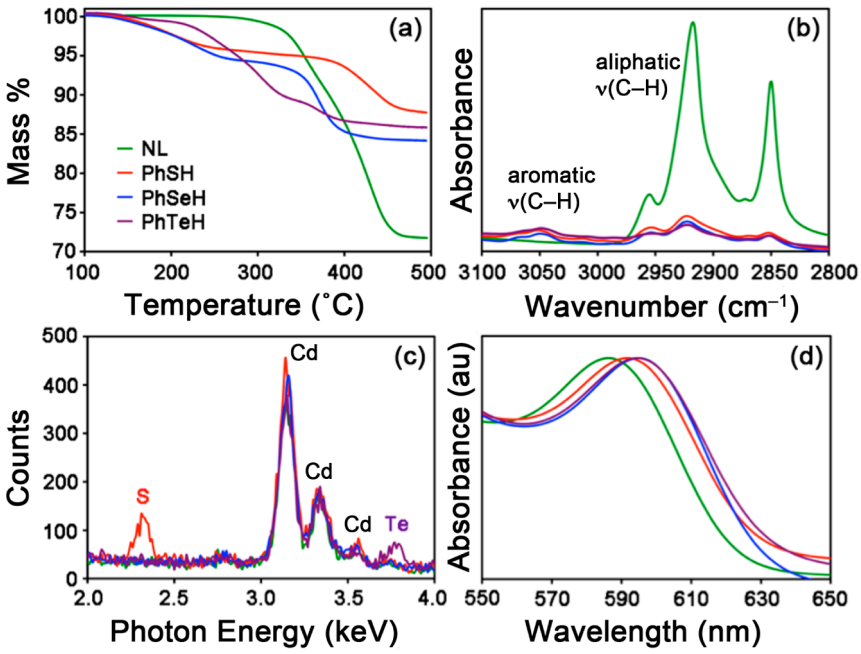

Figure 2. Thermogravimetric and spectroscopic evidence for displacement of native ligands on the CdSe nanocrystal surface upon introduction of phenylchalcogenols. (a) TGA traces, (b) FT-IR spectra, (c) EDX spectra, and (d) UV−vis spectra of CdSe(NL) nanocrystals before (green data) and after ligand exchange with PhSH (red data), PhSeH (blue data), and PhTeH (purple data).

Statistical analysis, using a nonparametric Wilcoxon rank sum test (necessitated by the non-normal population distribution), of the nanocrystal diameters both before and after ligand exchange confirmed the increase in diameter (n = 1001; $p = 10^{-142}$). Size histograms comparing the two sets of nanocrystals (*i.e.*, native ligand and tellurol-exchanged) help to visualize the increase by showing a clear shift to larger diameters for the tellurol-exchanged CdSe nanocrystals (see the Supporting Information, Figure S9). To further verify the statistical significance of the size increase from ligand exchange, a box plot representation of the data clearly shows that the notched regions do not overlap, indicating with 95% confidence that the true median diameters are significantly different. Quantification of the increase showed that after ligand exchange with PhTeH, the mean diameter of the CdSe nanocrystals increased by ~0.7 nm to 4.6 ± 0.5 nm. Likewise, ligand exchange with ^{t}BuTeH resulted in an increase in mean diameter by ~0.9 nm to 4.8 ± 0.8 nm. The increase in nanocrystal size after addition of the tellurol ligands is roughly consistent with the addition of a monolayer of tellurium to the nanocrystal surface, assuming an ionic radius of 0.21 nm for Te^{2-} (*i.e.*, 4 × 0.21 nm =0.84 nm).

Photophysical Measurements. Due to their widespread use, the influence of thiols on the photophysical properties of CdSe nanocrystals has been thoroughly investigated. The current study employs PhSH as a benchmark while investigating the effect of the lesser-known selenol and tellurol ligands on the photophysical properties of CdSe nanocrystals. In colloidal nanocrystals, several processes are known to induce relaxation to the ground state. They have been identified as radiative relaxation (band-edge emission), Auger nonradiative scattering,[42] Förster energy transfer to bigger nanocrystals, thermal escape,[43−45] trapping in surface and/or defects states,[32,43,46−49] and ligand-induced charge transfer.[31,32,46,49,50] The large number of identified processes, together with the intrinsic size and surface chemistry distribution of samples, typically results in complex decay profiles. Here, by performing time-resolved photoluminescence measurements at low excitation densities, concentrations, and temperatures, we reduce the influence of some of these processes (namely, Auger nonradiative scattering, Förster energy transfer, and thermal escape) in order to focus on the ligand influence on excited state dynamics of CdSe nanocrystals. Finally, surface state trapping can be studied at low temperature thanks to a broad, sub-band gap emission band that appears below 650 nm in CdSe nanocrystals. It is associated with relaxation of the electron or hole to surface states, followed by emissive, sub-band gap recombination. The surface states implicated are either selenium[46] or cadmium vacancies[47] (*i.e.*, Cd or Se dangling bonds, respectively). Historically, CdSe nanocrystals exhibited sub-band gap emission even at room temperature; progress in surface passivation has succeeded in reducing this emission as a result of core−shell[32,43] and/or ligand engineering.[46,48]

The optical properties of the ligand exchanged CdSe nanocrystals were investigated by UV−vis absorption and PL spectroscopies. The samples were dispersed in toluene (native ligands) or TMU (phenylchalcogenol ligands) and prepared such that they had similar absorbances. All of the absorbance spectra exhibit a bathochromic shift of the first exciton peak relative to

CdSe(NL) after ligand exchange, with the phenylchalcogenol ligands causing a red shift following the general trend S < Se ≤ Te (Figure 2d). For example, the first exciton peak was red-shifted by 22 meV after ligand exchange with PhSH, while ligand exchange with either PhSeH or PhTeH both resulted in a 32 meV red shift relative to CdSe(NL). Bathochromic shifts (<40 meV) in the optical absorbance spectra of CdSe quantum dots are commonly observed upon adsorption of thiol ligands.[46] The effect is attributed to the relaxed quantum confinement resulting from the coupling between the HOMOs of the thiol and the orbitals of the CdSe valence band.[51,52] Here, the quantum confinement is further relaxed for PhSeH and PhTeH ligands compared to the PhSH. This enhanced stabilization is related to increased delocalization of the hole wave function into the Se and Te ligand binding group, as discussed below. Equivalently, in a finite quantum well picture, the stabilization is due in part to the size increase observed by TEM (spatial relaxation of the quantum confinement by increasing the size of the well) and also to the modification of the energetic and dielectric environment[53] of the nanocrystal (*i.e.*, energetic relaxation of the quantum confinement by lowering the height of the energy barrier). Interestingly, red shifts of the first exciton peak were also observed for the different R groups in our study, with increasing red-shifts following the trend ^{t}BuSeH < BnSeH < PhSeH (see the Supporting Information, Figure S10). This trend likely corresponds to the increasingly proximal aromatic ring to the nanocrystals.

The photoluminescence of CdSe nanocrystals is red-shifted relative to the first excitonic feature in absorption because of the fine structure of the lowest exciton state.[42] Interestingly, ligand exchange with phenylchalcogenols results in greater red-shifts for the emission maxima than for the exciton absorbance (Figure 3a); the native ligand capped nanocrystals emit at 601 nm, while the PhSH-capped nanocrystals emit at 615 nm, and the PhSeH- and PhTeH-capped nanocrystals emit at 619 nm, corresponding to shifts by 44 and 57 meV relative to the CdSe(NL) emission, respectively. The greater shifts observed in emission compared to those observed in absorption reveal that the magnitude of the exciton fine structure splitting depends on the surface ligands; the dark exciton (observed in photoluminescence) is more stabilized by ligand exchange than the bright exciton (observed in absorbance). While the Stokes shift is known to be size dependent,[54] the expected size effect is much smaller than that observed here. The exciton fine structure splitting depends on the electron and hole wave function overlap and on the dielectric surroundings of the nanocrystals,[42] and therefore is expected to be ligand dependent.

Not surprisingly, the PL intensity is also greatly affected by the ligand exchange. The steady-state photoluminescence spectra of CdSe nanocrystals ligated either with stearate or exchanged with phenylchalcogenols

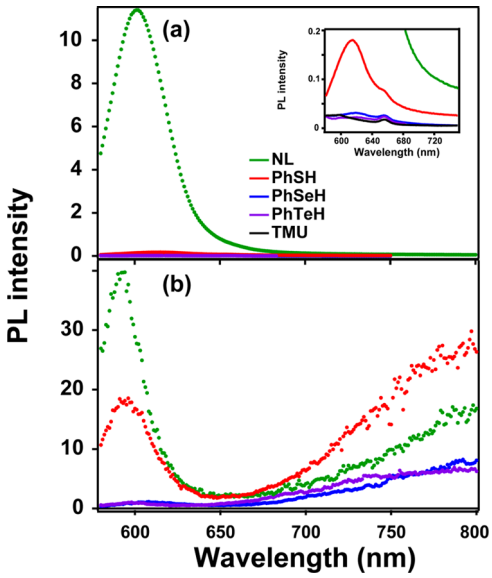

Figure 3. Steady-state PL spectra of CdSe nanocrystals suspended in toluene (native ligands) or TMU (phenylchalcogenol ligands). (a) Room temperature steady-state PL spectra of CdSe(NL) nanocrystals before (green data) and after ligand exchange with PhSH (red data), PhSeH (blue data), and PhTeH (purple data) with λ_{ex} = 550 nm. The PL intensities have been normalized by the absorbances at the excitation wavelength to account for slight differences in concentration (absorbances = 0.1−0.2 OD). The inset shows a zoom of the phenychalcogenol-exchanged nanocrystals. (b) Low temperature (77 K) steady-state PL spectra of CdSe(NL) nanocrystals before (green data) and after ligand exchange with PhSH (red data), PhSeH (blue data), and PhTeH (purple data) with λ_{ex} = 550 nm. As a result of the intense PL signals at 77 K, dilute suspensions were used (absorbances = 2 × 10^{-2} OD).

clearly show that the ligand exchange results in strong PL quenching for all three phenylchalcogenol ligands (Figure 3a). Control experiments performed with neat PhSeH *vs* PhSeH and Ph_2PH show comparable quenching in the absence of Ph_2PH, suggesting that the phosphine does not play a role in the observed PL quenching (see the Supporting Information, Figure S11). Additionally, control experiments run to determine the effect of ligand concentration on the PL quenching show that the PL quenching was not dependent on the concentration of added ligand in the saturated regime (*i.e.*, 0.018 mmol Ph_2Se_2/mg CdSe) used in this study (see the Supporting Information, Figure S12). While this experimental evidence points to the conclusion that ligand coverage may not be the determining factor in the PL quenching, it is still difficult to definitively rule out this effect. Thiol ligands are well-known to introduce midgap hole traps in CdSe nanocrystals, resulting in strong quenching of the photoluminescence.[31,32,46,52,53] The thiol ligands attract the hole and reduce its wave function overlap with the excitonic electron counterpart, thereby reducing the coupling between electron and hole and their emissive recombination. Interestingly, the PL quenching is even stronger in the case of PhSeH and PhTeH ligands. This observation is consistent with our DFT calculations of the phenylchalcogenol ligand energy levels (vacuum, basis

B3LYP-LACVP**, see the Supporting Information, Table S2). These calculations suggest that PhSeH and PhTeH possess higher lying HOMO levels than the PhSH. They can therefore also act as excitonic hole traps, possibly with a larger driving force for hole transfer than the PhSH ligands. The species created by hole transfer to the phenylchalcogenol ligands are not emissive in the detected energy range, as shown by the absence of PL signal below the band gap energy of the nanocrystals and down to 1.55 eV (800 nm).

The mechanism of PL quenching *via* hole transfer to the chalcogenol ligands can be further investigated by time-resolved PL measurements. At low temperature in particular, the influence of phonons is reduced, leading to a clearer view of the hole transfer dynamics. Indeed, time-resolved PL measurements at 77 K show that the band-edge PL is quenched rapidly in all ligand exchanged nanocrystals (Figure 4b). While the PL signal of PhSH-capped nanocrystals also exhibit a long-lived component, both PhSeH- and PhTeH-capped nanocrystals are almost entirely quenched. The characteristic time for hole quenching is close to the time resolution of the TCSPC apparatus for all phenylchalcogenol ligands; in the case of PhSH, the decay can be fitted with a 40 ps component, while in the case of PhSeH and PhTeH, the fast characteristic time for hole transfer is smaller than the time resolution (30 ps, see the Supporting Information, Table S3). At longer times, all samples exhibit a slow decay component with a characteristic lifetime on the order of 1 ns, similar to what is observed in the CdSe(NL) sample; however, this component is of much smaller relative amplitude for PhSeH and PhTeH than for PhSH and NL capped nanocrystals.

At room temperature, all phenylchalcogenol-exchanged CdSe nanocrystals exhibit a similar, instrument-limited decay component (Figure 4a) that arises from a combination of hole transfer to the chalcogenol ligand and of phonon-assisted nonradiative decay pathways. In effect, phonon-assisted relaxation can be assessed by comparing the PL decay dynamics of the nanocrystals capped with native ligands at room temperature (Figure 4a) and at 77 K (Figure 4b). At room temperature, the PL is rapidly quenched with a characteristic time around 60 ps (see the Supporting Information, Table S3). This fast component is not present in the 77 K PL decay, so it is attributed to phonon-assisted relaxation. The quenching for nanocrystals with PhSH ligands is faster at room temperature than at 77 K, suggesting that hole transfer to the ligands could be thermally activated.

Finally, all the nanocrystals presented in this study exhibit a long-lived sub-band gap emission at 77 K (lifetime determined to be longer than 100 μs from the inverse repetition rate of the pulse LED illumination source used for these measurements; data not shown) attributed to surface state trapping (Figure 3b).[46,47]

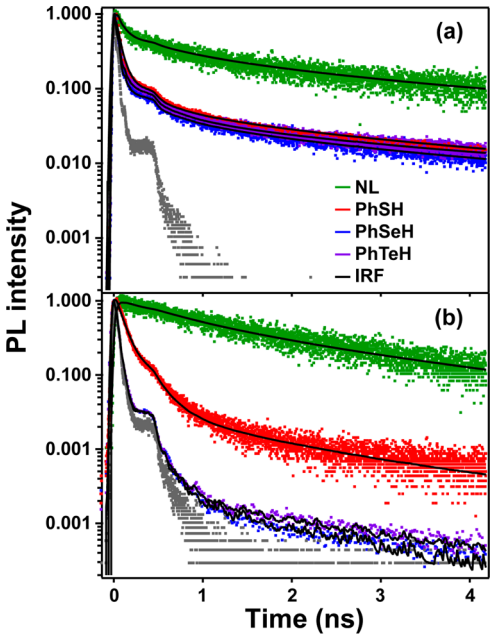

Figure 4. Time-resolved PL spectra of CdSe nanocrystals suspended in toluene (native ligands) or TMU (exchanged ligands). (a) Room temperature time-resolved PL spectra of CdSe(NL) nanocrystals before (green data, λ_{em} = 605 nm) and after ligand exchange with PhSH (red data, λ_{em} = 614 nm), PhSeH (blue data, λ_{em} = 619 nm), and PhTeH (purple data, λ_{em} = 620 nm) with λ_{ex} = 550 nm. (b) Low temperature (77 K) time-resolved PL spectra of CdSe(NL) nanocrystals before (green data, λ_{em} = 590 nm) and after ligand exchange with PhSH (red data, λ_{em} = 592 nm), PhSeH (blue data, λ_{em} = 591 nm) and PhTeH (purple data, λ_{em} = 601 nm). All signals have been normalized to their maximum intensity. The black curves show the fits to the data. The TCSPC apparatus instrument response function (IRF) is given in gray.

Interestingly, the exchange with PhSH resulted in an increase of the surface state emission intensity relative to the native ligands. This observation is consistent with the literature. Baker and Kamat attribute the increase of surface state emission to selenium vacancies; the exchange with thiols is thought to result in strong Cd−S bonds, which weaken the surface Cd−Se bonds and facilitate Se oxidation and increase the number of selenium vacancies and the intensity of surface state emission.[46] Here, in the case of the PhSeH and PhTeH, the surface state emission intensity is reduced relative to the native ligands. This set of observations can be explained by different scenarios and we think that experimental evidence is lacking to strictly attribute surface state trapping to electron or to hole trapping, *i.e.*, to Cd dangling bonds or Se dangling bonds, respectively. Both cases could lead to our observations. In the case of electron trapping, the increase in surface state emission intensity after thiol exchange could arise from surface Se oxidation, as in the work of Baker and Kamat—an effect that would be smaller for Se and Te ligands due to weaker binding strengths with surface Cd atoms. In the case of surface hole trapping, the highly effective hole transfer to the

PhSeH and PhTeH ligands, discussed above, could compete with the surface state hole trapping, while the less efficient hole transfer to PhSH would not.

In summary, band-edge emission in phenylchalcogenol-exchanged quantum dots is a competition between (i) radiative relaxation; (ii) hole transfer to the ligands (at 77 K, 40 ps for PhSH, < 30 ps for PhSeH and PhTeH); (iii) surface state trapping, detectable *via* a broad, long-lived sub-band gap emission at 77 K; and (iv) phonon-assisted nonradiative decay pathways at room temperature (~60 ps). The PhSeH and PhTeH ligands appear to be more efficient hole acceptors than PhSH ligands. This finding shows that, contrary to intuition, adding Se atoms to the quantum dots by ligand engineering does not simply make the nanocrystals "larger" from the PL decay point of view. Mixed coverage of the surface of nanocrystals by ligands with different end groups (alkyl chains from native ligands and phenyl groups from exchanged ligands in this case) leads to inhomogeneous Se or Te shell growth and creates very effective hole-transfer pathways. In particular, we suggest that hole transfer processes could effectively compete with hole surface state trapping (followed by emission of a photon) for selenol and tellurol ligands. Finally, while hole transfer to thiol ligands reduces the band-edge PL lifetime, it has been shown to increase the ground state depopulation lifetime in transient absorption measurements of thiol-capped CdSe nanocrystals.[50] Therefore, in the context of solar energy conversion, hole transfer to the ligand could be a way to delay energy relaxation; efficient hole quenchers such as selenol or tellurol ligands could become the first step to extract energy from the system, through a cascade of charge transfers whereby the holes are spatially pulled away from electrons.

CONCLUSIONS

We report a generalized strategy for the colloidal ligand exchange of CdSe nanocrystals with chalcogenol ligands. This approach utilizes simple reduction chemistry to yield a range of small chalcogenol ligands, a number of which were previously unreported, by using a variety of dialkyl and diaryl dichalcogenides as precursors. The ligand exchanged CdSe nanocrystals show on average an 80% decrease in native ligand content and maintain high colloidal stability in a number of moderately polar solvents, despite the small size of the new ligands. The temperature-dependent PL spectra and PL lifetime measurements on phenylchalcogenol-exchanged CdSe nanocrystals showed that the competition between band-edge emission, surface state trapping, phonon-assisted nonradiative relaxation pathways, and hole transfer tunes the amplitudes of the PL signals and their relaxation rates. Importantly, we showed that selenol and tellurol-based ligands on CdSe nanocrystals induce more efficient hole transfer than thiol-based ligands.

EXPERIMENTAL METHODS

General Considerations. The following chemicals were used as received without further purification. $CdCO_3$ (99.998% metals basis, "Puratronic" grade, Alfa Aesar), selenium (200 mesh powder, 99.999% metals basis, Alfa Aesar), tri-*n*-octylphosphine oxide (TOPO, 98%, Alfa Aesar), tri-*n*-octylphosphine (TOP, ≥97%, Strem), stearic acid (95%, Sigma-Aldrich), diphenyldisulfide (Ph_2S_2, 98%, TCI America), diphenyldiselenide (Ph_2Se_2, 98%, Strem), diphenylditelluride (Ph_2Te_2, 98%, Aldrich), dibenzyldisulfide (Bn_2S_2, 98+%, Alfa Aesar), dibenzyldiselenide (Bn_2Se_2, 95%, Alfa Aesar), diphenylphosphine (Ph_2PH, 98%, Sigma-Aldrich). Di-*tert*-butyldiselenide ($^tBu_2Se_2$) was synthesized using a literature procedure.[55] Di-*tert*-butylditelluride ($^tBu_2Te_2$) was also synthesized using a literature procedure.[56] Tetramethylurea (TMU, 99%, Alfa Aesar) was distilled at atmospheric pressure under nitrogen before use, discarding ~5−10% residue in the distillation flask. Deuterated NMR solvents were purchased from Cambridge Isotopes Laboratories and used as received.

Ligand Exchange Procedure. All ligand exchanges were performed using the following procedure in 23 mL vials under nitrogen. R_2E_2 (0.30 mmol) was added to 17 mg of CdSe(NL) nanocrystals dispersed in 1 mL of toluene. This solution was purged with nitrogen for 5 min while stirring, followed by the addition of Ph_2PH (171 mg, 0.920 mmol). Regardless of the R_2E_2 precursor used, the reaction was allowed to stir for 24 h. The exchanged CdSe nanocrystals were purified by flocculation with pentane (6 mL), followed by centrifugation (6000 rpm, 1 min). After each washing step, the particles were redispersed in TMU (0.5 mL). This procedure was repeated four times to ensure removal of all free ligands.

Material Characterization. TGA measurements were made on a TA Instruments TGA Q50 instrument, using sample sizes of ~5 mg in an alumina crucible under a flowing nitrogen atmosphere. TGA samples were prepared by fully drying the colloid under flowing nitrogen at 100 °C for 30 min prior to analysis. FT-IR spectra were recorded on a Bruker Vertex 80. To obtain quantitative data, an internal standard ($Fe_4[Fe(CN)_6]_3$, Alfa Aesar) was used according to a known procedure.[25] UV−vis spectra were acquired on a Shimadzu UV-1800 spectrophotometer using a quartz cuvette. TEM was performed on a JEOL JEM-2100 microscope at an operating voltage of 200 kV, equipped with a Gatan Orius CCD camera. Samples were prepared from dilute purified dispersions and deposited onto 300 mesh Formvar-coated copper grids (Ted Pella, Inc.). ^1H, ^{31}P and ^{77}Se NMR spectra were obtained on a Varian 500 spectrometer (500 MHz in ^1H, 202 MHz in ^{31}P, 95 MHz in ^{77}Se) with chemical shifts reported in units of ppm. All ^1H chemical shifts are referenced to the residual ^1H solvent (relative to TMS). EDX spectra were collected on a JEOL JSM-6610 scanning electron microscope operating at 10 kV equipped with an EDAX Apollo silicon drift detector (SDD). Multiple regions of a sample deposited on an aluminum stub were analyzed. PL spectra were collected on a Horiba Jobin Yvon Nanolog spectrofluorimeter system equipped with a 450 W Xe lamp as the excitation source and a photomultiplier tube as the detector. The excitation wavelength was 550 nm for all measurements. The samples were placed in a standard 1-cm path length quartz cuvette for the room temperature measurements. For low temperature (77 K) PL measurements, a liquid nitrogen-cooled Dewar was used and the samples were placed in an NMR tube.

PL Lifetime Studies. TCSPC measurements (30 ps time resolution) were performed using a R3809U-50 Hamamatsu PMT with a B&H SPC-630 module. Samples were excited with the 550 nm output of an OPA, pumped by a Ti:sapphire regenerative amplifier operating at 250 kHz (Coherent RegA 9050). Laser pulses were focused into the sample using a 15 cm focal lens, with illumination powers between 3.2 mW and

1.5 μW. Emission was collected at the emission peak of the nanocrystals at magic angle polarization relative to the 550 nm excitation. The emission was collimated and then focused into a monochromator with a 10 cm lens. The monochromator was a CVI CMSP112 double spectrograph with a 1/8 m total path length in negative dispersive mode with a 600 g mm^{-1} grating blazed at 600 nm. The slit widths were 1.2 mm, resulting in a 20 nm resolution.

Samples were dispersed in toluene (for the CdSe(NL) nanocrystals) or TMU (for the phenylchalcogenol-exchanged CdSe nanocrystals) to obtain optical densities between 0.1 and 0.2 OD at the excitation wavelength; cuvettes or NMR tubes were used for room temperature and 77 K measurements, respectively, as explained above. The excitation fluences, between 40 μJ cm^{-2} and 20 nJ cm^{-2}, were chosen depending on the strength of the photoluminescence signal (*i.e.*, depending on the ligands and on the temperature), so that excitation resulted in less than one excited electron–hole pair per nanocrystal.[52,53]

Attempts were made to measure the lifetime of the longer wavelength sub-band gap emission of the nanocrystals at 77 K by using a IBH Fluorocube instrument equipped with a 405 nm LED excitation source at a 10 kHz repetition rate. Although signal was detected, the extremely long-lived sample luminescence decayed more slowly than the LED source repetition rate making a quantitative determination of lifetime impossible.

Conflict of Interest: The authors declare no competing financial interest.

Acknowledgment. The ligand exchange chemistry is based on work supported by the National Science Foundation under DMR-1205712. M.J.G., E.C. and S.E.B., as well as the photophysics work, were supported as part of the Center for Energy Nanoscience, an Energy Frontier Research Center funded by the U.S. Department of Energy, Office of Science, Office of Basic Energy Sciences, under Award No. DE-SC0001013. R.L.B. acknowledges the Research Corporation for Science Advancement for a Cottrell Scholar Award and J.J.B. acknowledges the National Science Foundation for a Graduate Research Fellowship. J.M.'s participation in a summer undergraduate research program was supported by NSF CHE-0957868 to S.E.B. The authors would like to thank D. Webber for his artistic contribution to the TOC graphic.

Supporting Information Available: NMR spectra with assignments, supplemental TGA, PL, and TEM data. This material is available free of charge *via* the Internet at http://pubs.acs.org.

REFERENCES AND NOTES

1. Pokrant, S.; Whaley, K. B. Tight-Binding Studies of Surface Effects on Electronic Structure of CdSe Nanocrystals: The Role of Organic Ligands, Surface Reconstruction, and Inorganic Capping Shells. *Eur. Phys. J. D* **1999**, *6*, 255–267.
2. Bullen, C.; Mulvaney, P. The Effects of Chemisorption on the Luminescence of CdSe Quantum Dots. *Langmuir* **2006**, *22*, 3007–3013.
3. Jasieniak, J.; Mulvaney, P. From Cd-Rich to Se-Rich—The Manipulation of CdSe Nanocrystal Surface Stoichiometry. *J. Am. Chem. Soc.* **2007**, *129*, 2841–2848.
4. Luther, J. M.; Pietryga, J. M. Stoichiometry Control in Quantum Dots: A Viable Analog to Impurity Doping of Bulk Materials. *ACS Nano* **2013**, *7*, 1845–1849.
5. Talapin, D. V.; Lee, J.-S.; Kovalenko, M. V.; Shevchenko, E. V. Prospects of Colloidal Nanocrystals for Electronic and Optoelectronic Applications. *Chem. Rev.* **2009**, *110*, 389–458.
6. Zabet-Khosousi, A.; Dhirani, A. A. Charge Transport in Nanoparticle Assemblies. *Chem. Rev.* **2008**, *108*, 4072–4124.
7. Sargent, E. H. Solar Cells, Photodetectors, and Optical Sources from Infrared Colloidal Quantum Dots. *Adv. Mater.* **2008**, *20*, 3958–3964.
8. Tang, J.; Sargent, E. H. Infrared Colloidal Quantum Dots for Photovoltaics: Fundamentals and Recent Progress. *Adv. Mater.* **2011**, *23*, 12–29.
9. Taylor, J.; Kippeny, T.; Rosenthal, S. J. Surface Stoichiometry of CdSe Nanocrystals Determined by Rutherford Backscattering Spectroscopy. *J. Cluster Sci.* **2001**, *12*, 571–582.
10. Morris-Cohen, A. J.; Donakowski, M. D.; Knowles, K. E.; Weiss, E. A. The Effect of a Common Purification Procedure on the Chemical Composition of the Surfaces of CdSe Quantum Dots Synthesized with Trioctylphosphine Oxide. *J. Phys. Chem. C* **2010**, *114*, 897–906.
11. Anderson, N. C.; Hendricks, M. P.; Choi, J. J.; Owen, J. S. Ligand Exchange and the Stoichiometry of Metal Chalcogenide Nanocrystals: Spectroscopic Observation of Facile Metal-Carboxylate Displacement and Binding. *J. Am. Chem. Soc.* **2013**, *135*, 18536–18548.
12. Fritzinger, B.; Capek, R. K.; Lambert, K.; Martins, J. C.; Hens, Z. Utilizing Self-Exchange To Address the Binding of Carboxylic Acid Ligands to CdSe Quantum Dots. *J. Am. Chem. Soc.* **2010**, *132*, 10195–10201.
13. Anderson, N. C.; Owen, J. S. Soluble, Chloride-Terminated CdSe Nanocrystals: Ligand Exchange Monitored by ^{1}H and ^{31}P NMR Spectroscopy. *Chem. Mater.* **2012**, *25*, 69–76.
14. Fafarman, A. T.; Koh, W.-k.; Diroll, B. T.; Kim, D. K.; Ko, D.-K.; Oh, S. J.; Ye, X.; Doan-Nguyen, V.; Crump, M. R.; Reifsnyder, D. C.; *et al.* Thiocyanate-Capped Nanocrystal Colloids: Vibrational Reporter of Surface Chemistry and Solution-Based Route to Enhanced Coupling in Nanocrystal Solids. *J. Am. Chem. Soc.* **2011**, *133*, 15753–15761.
15. Nag, A.; Kovalenko, M. V.; Lee, J. S.; Liu, W. Y.; Spokoyny, B.; Talapin, D. V. Metal-free Inorganic Ligands for Colloidal Nanocrystals: S^{2-}, HS^{-}, Se^{2-}, HSe^{-}, Te^{2-}, HTe^{-}, TeS_3^{2-}, OH^{-}, and NH_2^{-} as Surface Ligands. *J. Am. Chem. Soc.* **2011**, *133*, 10612–10620.
16. Zhang, H.; Hu, B.; Sun, L.; Hovden, R.; Wise, F. W.; Muller, D. A.; Robinson, R. D. Surfactant Ligand Removal and Rational Fabrication of Inorganically Connected Quantum Dots. *Nano Lett.* **2011**, *11*, 5356–5361.
17. Liu, I. S.; Lo, H.-H.; Chien, C.-T.; Lin, Y.-Y.; Chen, C.-W.; Chen, Y.-F.; Su, W.-F.; Liou, S.-C. Enhancing Photoluminescence Quenching and Photoelectric Properties of CdSe Quantum Dots with Hole Accepting Ligands. *J. Mater. Chem.* **2008**, *18*, 675–682.
18. Kovalenko, M. V.; Scheele, M.; Talapin, D. V. Colloidal Nanocrystals with Molecular Metal Chalcogenide Surface Ligands. *Science* **2009**, *324*, 1417–1420.
19. Dong, A.; Ye, X.; Chen, J.; Kang, Y.; Gordon, T.; Kikkawa, J. M.; Murray, C. B. A Generalized Ligand-Exchange Strategy Enabling Sequential Surface Functionalization of Colloidal Nanocrystals. *J. Am. Chem. Soc.* **2011**, *133*, 998–1006.
20. Rosen, E. L.; Buonsanti, R.; Llordes, A.; Sawvel, A. M.; Milliron, D. J.; Helms, B. A. Exceptionally Mild Reactive Stripping of Native Ligands from Nanocrystal Surfaces by Using Meerwein's Salt. *Angew. Chem., Int. Ed.* **2012**, *51*, 684–689.
21. Murray, C. B.; Norris, D. J.; Bawendi, M. G. Synthesis and Characterization of Nearly Monodisperse CdE (E = Sulfur, Selenium, Tellurium) Semiconductor Nanocrystallites. *J. Am. Chem. Soc.* **1993**, *115*, 8706–8715.
22. Porter, V. J.; Geyer, S.; Halpert, J. E.; Kastner, M. A.; Bawendi, M. G. Photoconduction in Annealed and Chemically Treated CdSe/ZnS Inorganic Nanocrystal Films. *J. Phys. Chem. C* **2008**, *112*, 2308–2316.
23. Johnston, K. W.; Pattantyus-Abraham, A. G.; Clifford, J. P.; Myrskog, S. H.; MacNeil, D. D.; Levina, L.; Sargent, E. H. Schottky-Quantum Dot Photovoltaics for Efficient Infrared Power Conversion. *Appl. Phys. Lett.* **2008**, *92*, 151115.
24. Lokteva, I.; Radychev, N.; Witt, F.; Borchert, H.; Parisi, J.; Kolny-Olesiak, J. Surface Treatment of CdSe Nanoparticles for Application in Hybrid Solar Cells: The Effect of Multiple Ligand Exchange with Pyridine. *J. Phys. Chem. C* **2010**, *114*, 12784–12791.
25. Webber, D. W.; Brutchey, R. L. Ligands Exchange on Colloidal CdSe Nanocrystals Using Thermally Labile *tert*-Butylthiol for Improved Photocurrent in Nanocrystal Films. *J. Am. Chem. Soc.* **2012**, *134*, 1085–1092.
26. Greaney, M. J.; Das, S.; Webber, D. H.; Bradforth, S. E.; Brutchey, R. L. Improving Open Circuit Potential in Hybrid P3HT:CdSe Bulk Heterojunction Solar Cells *via* Colloidal

tert-Butylthiol Ligand Exchange. *ACS Nano* **2012**, *6*, 4222–4230.
27. Greaney, M. J.; Araujo, J.; Burkhart, B.; Thompson, B. C.; Brutchey, R. L. Novel Semi-Random and Alternating Copolymer Hybrid Solar Cells Utilizing CdSe Multipods as Versatile Acceptors. *Chem. Commun.* **2013**, *49*, 8602–8604.
28. Schapotschnikow, P.; Hommersom, B.; Vlugt, T. J. H. Adsorption and Binding of Ligands to CdSe Nanocrystals. *J. Phys. Chem. C* **2009**, *113*, 12690–12698.
29. Munro, A. M.; Plante, I. J.-L.; Ng, M. S.; Ginger, D. S. Quantitative Study of the Effects of Surface Ligand Concentration on CdSe Nanocrystal Photoluminescence. *J. Phys. Chem. C* **2007**, *111*, 6220–6227.
30. Steigerwald, M. L.; Alivisatos, A. P.; Gibson, J. M.; Harris, T. D.; Kortan, R.; Muller, A. J.; Thayer, A. M.; Duncan, T. M.; Douglass, D. C.; Brus, L. E. Surface Derivatization and Isolation of Semiconductor Cluster Molecules. *J. Am. Chem. Soc.* **1988**, *110*, 3046–3050.
31. Knowles, K. E.; Tice, D. B.; McArthur, E. A.; Solomon, G. C.; Weiss, E. A. Chemical Control of the Photoluminescence of CdSe Quantum Dot−Organic Complexes with a Series of Para-Substituted Aniline Ligands. *J. Am. Chem. Soc.* **2010**, *132*, 1041–1050.
32. Munro, A. M.; Jen-La Plante, I.; Ng, M. S.; Ginger, D. S. Quantitative Study of the Effects of Surface Ligand Concentration on CdSe Nanocrystal Photoluminescence. *J. Phys. Chem. C* **2007**, *111*, 6220–6227.
33. Hughes, B. K.; Ruddy, D. A.; Blackburn, J. L.; Smith, D. K.; Bergren, M. R.; Nozik, A. J.; Johnson, J. C.; Beard, M. C. Control of PbSe Quantum Dot Surface Chemistry and Photophysics Using an Alkylselenide Ligand. *ACS Nano* **2012**, *6*, 5498–5506.
34. Qu, L.; Peng, A.; Peng, X. Alternative Routes toward High Quality CdSe Nanocrystals. *Nano Lett.* **2001**, *1*, 333–337.
35. Jasieniak, J.; Smith, L.; Embden, J. v.; Mulvaney, P. Re-examination of the Size-Dependent Absorption Properties of CdSe Quantum Dots. *J. Phys. Chem. C* **2009**, *113*, 19468–19474.
36. Hens, Z.; Martins, J. C. A Solution NMR Toolbox for Characterizing the Surface Chemistry of Colloidal Nanocrystals. *Chem. Mater.* **2013**, *25*, 1211–1221.
37. Gomes, R.; Hassinen, A.; Szczygiel, A.; Zhao, Q.; Vantomme, A.; Martins, J. C.; Hens, Z. Binding of Phosphonic Acids to CdSe Quantum Dots: A Solution NMR Study. *J. Phys. Chem. Lett.* **2011**, *2*, 145–152.
38. Tavasoli, E.; Guo, Y.; Kunal, P.; Grajeda, J.; Gerber, A.; Vela, J. Surface Doping Quantum Dots with Chemically Active Native Ligands: Controlling Valence without Ligand Exchange. *Chem. Mater.* **2012**, *24*, 4231–4241.
39. Crich, D.; Jiao, X.-Y.; Yao, Q.; Harwood, J. S. Radical Clock Reactions under Pseudo-First-Order Conditions Using Catalytic Quantities of Diphenyl Diselenide. A ^{77}Se- and ^{119}Sn-NMR Study of the Reaction of Tributylstannane and Diphenyl Diselenide. *J. Org. Chem.* **1996**, *61*, 2368–2373.
40. Sonoda, N.; Ogawa, A. Reagents for Radical and Radical Ion Chemistry Benzeneselenol. In *Handbook of Reagents for Organic Synthesis, Reagents for Radical and Radical Ion Chemistry*; Crich, D., Ed.; Wiley: Chichester, United Kingdom, 2008; p 39.
41. Kanicky, J. R.; Shah, D. O. Effect of Degree, Type, and Position of Unsaturation on the pK_a of Long-Chain Fatty Acids. *J. Colloid Interface Sci.* **2002**, *256*, 201–207.
42. Klimov, V. I.In *Handbook of Nanostructured Materials and Nanotechnology*; Academic Press: San Diego, CA, 2000; Vol. 4, Chap. 7.
43. Jing, P.; Zheng, J.; Ikezawa, M.; Liu, X.; Lv, S.; Kong, X.; Zhao, J.; Masumoto, Y. Temperature-Dependent Photoluminescence of CdSe-Core CdS/CdZnS/ZnS-Multishell Quantum Dots. *J. Phys. Chem. C* **2009**, *113*, 13545–13550.
44. Valerini, D.; Cretí, A.; Lomascolo, M.; Manna, L.; Cingolani, R.; Anni, M. Temperature Dependence of the Photoluminescence Properties of Colloidal CdSe/ZnS Core/Shell Quantum Dots Embedded in a Polystyrene Matrix. *Phys. Rev. B* **2005**, *71*, 235409.
45. Morello, G.; De Giorgi, M.; Kudera, S.; Manna, L.; Cingolani, R.; Anni, M. Temperature and Size Dependence of Nonradiative Relaxation and Exciton-Phonon Coupling in Colloidal CdTe Quantum Dots. *J. Phys. Chem. C* **2007**, *111*, 5846–5849.
46. Baker, D. R.; Kamat, P. V. Tuning the Emission of CdSe Quantum Dots by Controlled Trap Enhancement. *Langmuir* **2010**, *26*, 11272.
47. Underwood, D. F.; Kippeny, T.; Rosenthal, S. J. Ultrafast Carrier Dynamics in CdSe Nanocrystals Determined by Femtosecond Fluorescence Upconversion Spectroscopy. *J. Phys. Chem. B* **2001**, *105*, 436–443.
48. Wuister, S. F.; van Houselt, A.; de Mello Donega, C.; Vanmaekelbergh, D.; Meijerink, A. Temperature Antiquenching of the Luminescence from Capped CdSe Quantum Dots. *Angew. Chem., Int. Ed.* **2004**, *43*, 3029–3033.
49. Wuister, S. F.; de Mello Donega, C.; Meijerink, A. Influence of Thiol Capping on the Exciton Luminescence and Decay Kinetics of CdTe and CdSe Quantum Dots. *J. Phys. Chem. B* **2004**, *108*, 17393–17397.
50. Burda, C.; Link, S.; Mohamed, M.; El-Sayed, M. The Relaxation Pathways of CdSe Nanoparticles Monitored with Femtosecond Time-Resolution from the Visible to the IR: Assignment of the Transient Features by Carrier Quenching. *J. Phys. Chem. B* **2001**, *105*, 12286–12292.
51. Frederick, M. T.; Amin, V. A.; Weiss, E. A. Optical Properties of Strongly Coupled Quantum Dot-Ligand Systems. *J. Phys. Chem. Lett.* **2013**, *4*, 634–640.
52. Frederick, M. T.; Weiss, E. A. Relaxation of Exciton Confinement in CdSe Quantum Dots by Modification with a Conjugated Dithiocarbamate Ligand. *ACS Nano* **2010**, *4*, 3195–3200.
53. Piryatinski, A.; Ivanov, S. A.; Tretiak, S.; Klimov, V. I. Effect of Quantum and Dielectric Confinement on the Exciton−Exciton Interaction Energy in Type II Core/Shell Semiconductor Nanocrystals. *Nano Lett.* **2007**, *7*, 108–115.
54. Nirmal, M.; Norris, D. J.; Kuno, M.; Bawendi, M. G.; Efros, Al. L.; Rosen, M. Observation of the "Dark Exciton" in CdSe Quantum Dots. *Phys. Rev. Lett.* **1995**, *75*, 3728–3731.
55. Block, E.; Birringer, M.; Jiang, W.; Nakahodo, T.; Thompson, H.; Toscano, P. J.; Uzar, H.; Zhang, X.; Zhu, Z. Allium Chemistry: Synthesis, Natural Occurrence, Biological Activity, and Chemistry of Se-Alk(en)ylselenocysteines and Their γ-Glutamyl Derivatives and Oxidation Products. *J. Agric. Food Chem.* **2001**, *49*, 458–470.
56. Engman, L.; Cava, M. P. Organotellurium Compounds 5. A Convenient Synthesis of Some Aliphatic Ditellurides. *Synth. Commun.* **1982**, *12*, 163–165.